

STUDY OF ULTRA-HIGH ENERGY COSMIC RAYS FROM THE RADIO SIGNAL AT THE PIERRE AUGER OBSERVATORY

Jennifer Maller¹ and for the Pierre Auger Collaboration²

Abstract. Deployed at the end of 2010 at the Pierre Auger Observatory, the first stage of the Auger Engineering Radio Array, AERA24, consists of 24 radio stations covering an area of 0.5 km². AERA measures the radio emission from cosmic-ray induced air showers. The amplitude of this radio emission is used to constrain the characteristics of the primary particle: arrival direction, energy and nature. These studies are possible thanks to an instrumentation development allowing self-triggered and externally-triggered measurements in the MHz domain and an improved understanding of radio emission processes. In May 2013, 100 new stations were installed to cover an area of $\simeq 6$ km², for a total of 124 stations. This stage 2 will provide higher statistics and will enhance both the estimate of the nature of the primary cosmic ray and the energy resolution above 10¹⁷ eV as an addition to detectors such as the Auger fluorescence telescopes and particle detectors. We will present the main results obtained with the stage 1 of AERA and the current status of the experiment. We will end with a brief overview of the GHz-experiments installed at the Pierre Auger Observatory.

Keywords: AERA, radio detection, high energy cosmic rays, Pierre Auger Observatory

1 Introduction

One of the challenging questions related to cosmic rays concerns their nature. Improving our knowledge about the composition of cosmic rays allows us to constrain the models concerning their origins and their production mechanisms in the astrophysical sources. The electric field of radio emission induced by the shower is sensitive to the whole shower development and can be measured with a high duty cycle, and thus is a promising technique to identify observables sensitive to the nature of the primary cosmic ray.

In Europe two experiments have given the first modern results concerning the study of extensive air showers at low energy (because of their small area: less than 1 km²): CODALEMA (D. Ardouin et al. 2005) in France and LOPES (H. Falcke et al. 2005) in Germany.

The **Auger Engineering Radio Array** installed at the Pierre Auger Observatory has recently been extended and covers, with its stage 2 installed since the beginning of May 2013, approximately 6 km² with 124 radio stations. AERA allows the study of the radio emission during the development of the shower in the MHz domain. In this frequency range, two mechanisms lead to a polarized coherent radio signal.

The first one, **the geomagnetic effect** is due to the action of the geomagnetic field on the charged particles of the shower and leads to the creation of a linearly polarized electric field along the vector $-\mathbf{v} \times \mathbf{B}$. This phenomenon was described by Kahn and Lerche in 1966 (F. D. Kahn & I. Lerche 1966) and has been confirmed by several experiments.

The second one, **the charge excess effect**, was predicted by Askaryan in 1962 (G. A. Askaryan 1962) and is due to the annihilation of positrons in the shower and to the Compton effect leading to a negative charge excess in the shower front. It leads to the creation of a signal which is radially polarized with respect to the shower axis.

The main objective of AERA is to characterize the primary cosmic ray: nature, energy and arrival direction. For this it is necessary to disentangle the mechanisms responsible for the radio emission occurring during the

¹ Subatech, Université de Nantes, École des Mines de Nantes, CNRS/IN2P3, Nantes, France

² Pierre Auger Observatory, Av. San Martín Norte 304, 5613 Malargüe, Argentina
(Full author list : http://www.auger.org/archive/authors_2013.06.html)

development of the shower. This can be done by analyzing the polarization of the measured electric field as presented in section 2.2. AERA will also permit one to test the performances of a large radio array compared to the other techniques.

2 AERA - 1st stage

AERA is deployed in the low energy extension of the Pierre Auger Observatory in order to have a large statistics and high-quality super-hybrid measurements. It enables the comparison of radio observables with those obtained with the SD (regular and infill array) and the nine fluorescence telescopes close to AERA installed on both the HEAT and Coihueco sites. .

The stage 1 of AERA has operated at the observatory since 2010 and has taken taking data since 2011 with 24 stations spaced by 144 m and covering 0.5 km². Each station is equipped with:

- a Log Periodic Dipole Antenna measuring both EW and NS polarizations between 30 and 80 MHz,
- an electromagnetic compatibility box containing the electronics to prevent for the triggering of the station by itself,
- solar panels, batteries and GPS.

Thanks to this equipment AERA is completely autonomous in power supply and can also be used in a self-trigger mode for which the measured signal triggers the station if its level exceeds a predefined threshold. This defines the first level trigger T1. After a pulse-shape analysis performed directly at the station level, each station sends on average 500 level 2 triggers per second (T2). The corresponding timestamps are sent to the central data acquisition system. All T2s coming from all AERA stations are treated in real time to search for cosmic ray candidates studying the time difference between several pair of AERA stations event by event to check the compatibility of this event with the arrival of an air shower on the array. This is the level 3 trigger (T3).

AERA can also be externally triggered by the SD stations close to the array, and very soon by the fluorescence telescopes HEAT and Coihueco.

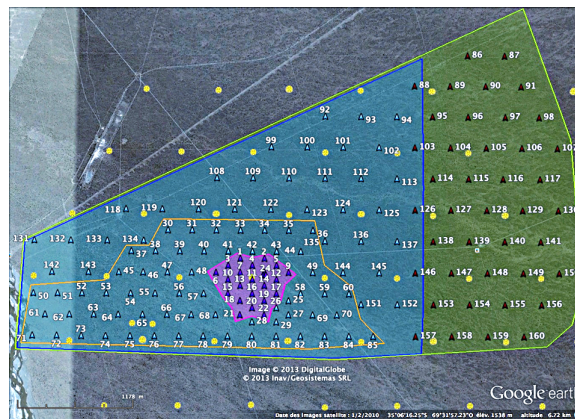


Fig. 1. AERA - In purple is shown the 1st stage with 24 stations, in blue are shown the 100 new stations of the 2nd stage installed since May 2013 and in green the last stations scheduled for 2014.

2.1 Proposed rejection algorithm

In the self-trigger mode the stations are mostly triggered by anthropic background and thunderstorms sending a huge number of T2s, occupying a large fraction of the bandwidth and saturating the disks. The background transients lower the detection efficiency of cosmic rays. To use this technique we must develop efficient rejection algorithms at level 1 or 2 of the trigger to increase the purity of the recorded signals.

We present here an example of such an algorithm which was developed for RAuger (B. Revenu for the Pierre Auger and CODALEMA Collaborations 2012), a prototype radio-detection experiment which was one of the pathfinders for AERA. The results of this prototype are described in (The Pierre Auger Collaboration,

S. Acounis, D. Charrier, T. Garçon, C. Rivière, & P. Stassi 2012b). The study presented here was performed using the data of the upgraded version of RAuger which was composed of three autonomous radio stations located near the Central Laser Facility at the center of the SD. These stations were equipped with Butterfly (D. Charrier for the CODALEMA Collaboration 2012) antennas developed for CODALEMA and are now equipping the stage 2 of AERA. The proposed selection algorithm has been established using two different data sets:

- air-shower events detected in coincidences between the RAuger stations and the SD stations close to the array,
- background events.

We study the time evolution of the filtered signal in a short time window containing the main pulse as illustrated in figure 2. In this time window and for each trace we sum up bin after bin the square of the amplitude of the signal to compute a normalized cumulative function. This cumulative function is defined as follows:

$$C(i) = \frac{\sum_{k=b_{start}}^{b_{start}+i} s_{EW}(k)^2}{\sum_{k=b_{start}}^{b_{end}} s_{EW}(k)^2}, \text{ with } 0 \leq i \leq b_{end} - b_{start}. \quad (2.1)$$

We have observed that, in most cases, a background trace has a longer duration than a cosmic ray trace. We define the rise time of the signal as the time needed for the cumulative function to rise from 10% to 70%. We observe (figure 3), that the rise time for cosmic rays (red triangles) is significantly smaller than the rise time of the background transients (black diamonds). The values 10% and 70% and the frequency range for the filtering (30-60 MHz) have been optimized for this experiment.

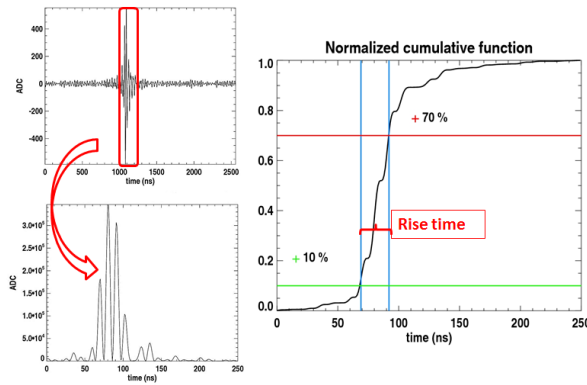


Fig. 2. Top-left: signal filtered in 30-60 MHz with the illustration of the used time window (in red) containing the main pulse; bottom-left: square of the filtered signal which is summed up bin after bin; right: cumulative function in black, the rise time (in red) is the time needed for the cumulative function to go from 10% (green line) to 70% (red line).

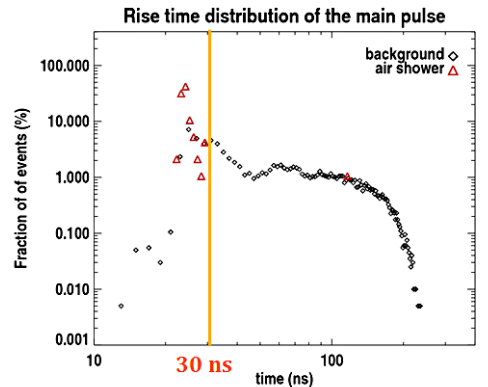


Fig. 3. Rise time distribution for two data sets: air shower events (red triangles) and background events (black diamonds). The upper limit cut on the rise time is set at 30 ns.

This rejection method has an efficiency of approximately 90% on the RAuger2 data (cut at 30 ns, orange line in figure 3). One cosmic ray trace is rejected by this method (isolated red triangle above 100 ns in figure 3). This signal is of very bad quality and is thus probably a random coincidence. The algorithm has been installed on CODALEMA since the beginning of 2013 with an efficiency of approximately 94% (D. Torres Machado for the CODALEMA Collaboration 2013) and is currently being tested on the AERA data.

2.2 Polarization studies

As discussed previously, the study of the polarization of the measured electric field allows a better understanding of the emission processes: several studies have confirmed the dominance of the geomagnetic effect (The Pierre Auger Collaboration et al. 2012b; D. Ardouin et al. 2012; M. Melissas for the Pierre Auger Collaboration

2012). These experiments have shown an excess of events coming from directions far from the direction of the geomagnetic field, which is a signature of the geomagnetic effect. When comparing the direction of the measured electric field with the expected direction due to this dominant mechanism ($-\mathbf{v} \times \mathbf{B}$) (K. Weidenhaupt for the Pierre Auger Collaboration 2012) as shown in figure 4, we observe some discrepancies which can indicate the presence of at least one other mechanism.

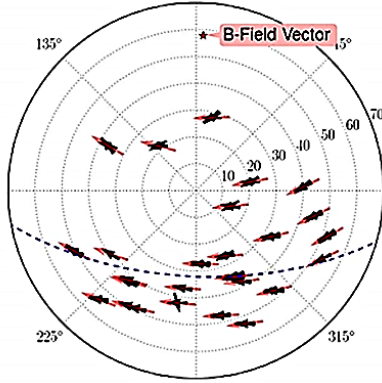


Fig. 4. Skymap showing the comparison between the direction of the measured electric field (in black) and the direction of $\mathbf{v} \times \mathbf{B}$ (in red). The geomagnetic field is shown with the red star.

The charge excess effect contributes to the secondary mechanism with a radial polarization contrary to that of the geomagnetic effect. To study the charge excess contribution, we define an R-parameter:

$$R = \frac{\sum_{i=1}^N E_x(t_i)E_y(t_i)}{\sum_{i=1}^N (E_x(t_i)^2 + E_y(t_i)^2)} \quad (2.2)$$

where the x axis (EW polarization) is aligned with the direction of $\mathbf{v} \times \mathbf{B}$ projected in the horizontal plane and the y axis (NS polarization) is perpendicular to x. By construction, $R = 0$ in the case of a pure geomagnetic emission. Thus, R measures the deviation from this effect.

We compare the R-parameter values obtained from the data to the values obtained using simulated data. For each event two simulations are performed: one includes only geomagnetic mechanism and the other one includes both mechanisms. The results presented in figure 5 have been obtained using the simulation code SELFAS2 (V. Marin & B Revenu 2012) but the same results hold with other simulation codes (T. Huege for the Pierre Auger Collaboration 2013) such as CoREAS (T. Huege et al. 2013), REAS3.1 (M. Ludwig & T. Huege 2011), EVA1.01 (K. Werner et al. 2012), ZHAires (J. Alvarez Muñiz et al. 2012) and MGMR (K. D. de Vries et al. 2012). The correlation is studied with the Pearson coefficient. We observe a much higher correlation level when both mechanisms are used in the simulation as shown in the left-figure. The phenomenon is thus much better described when we add a radial component in the polarization of the electric field, which is the main characteristic of the charge excess effect.

2.3 Energy estimation

The radio signal strength is strongly correlated to the primary cosmic ray characteristics, among them its energy. The results reported by RAuger (The Pierre Auger Collaboration et al. 2012b), CODALEMA (O. Ravel for the CODALEMA Collaboration 2012), LOPES (A. Horneffer for the LOPES Collaboration 2007) assume a radially symmetric lateral distribution function (LDF) as proposed in the past (H. R. Allan 1971), and show a linear dependence between the electric field strength and the primary energy. Preliminary results obtained by AERA (C. Glaser for Pierre Auger Collaboration 2013) are in good agreement with these observations. We now need more statistics which will be provided very soon by the stage 2 of the experiment. However, it has become clear (B Revenu 2013; A. Corstanje et al. 2011) that a 1D exponential LDF is not suited to the radio signal. More complicated 2D LDFs should be used for these analyses.

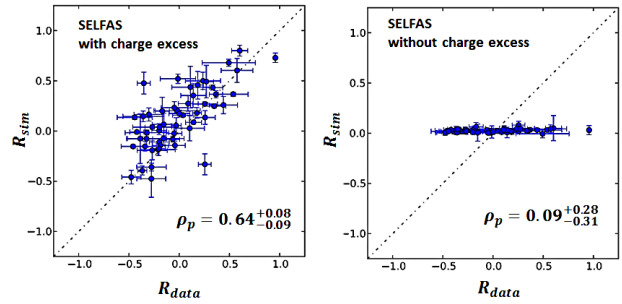


Fig. 5. Comparison between the R-parameter for data in abscissa with the R-parameter for two simulations: one performed with geomagnetic and charge excess effect (left) and another with only geomagnetic effect (right).

3 AERA - stage 2

The stage 2 of the experiment has been deployed at the observatory since May 2013 with 100 new stations covering 6 km² (blue part in figure 1), with two different grid sizes: 250 m for the stations included in the inner contour line and 375 m for the others. These new stations are equipped with Butterfly antennas (The Pierre Auger Collaboration et al. 2012a) which will provide a better sensitivity. Stage 2 will increase both the estimate of the nature and the energy resolution of the primary cosmic ray by the use of additional detectors. The final stage of AERA, scheduled for 2014, will be composed of 160 stations covering 12 km² (green part of the map shown in figure 1).

4 Conclusion

The study of high energy cosmic rays through the radio emission induced by air showers is a promising technique to identify observables sensitive to their characteristics and in particular to their nature, thanks to a high duty cycle and a sensitivity to the whole shower development.

The geomagnetic effect has been confirmed as the dominant mechanism and polarization studies together with simulations have highlighted the contribution of a radially polarized signal with respect to the transverse plane of the shower. This contribution could be interpreted as the charge excess effect.

The stage 1 of AERA has been taking data since 2011 with 24 radio stations running in self-trigger and external-trigger modes. The measurement of high energy cosmic rays by AERA and the additional detectors of the low energy extension could help study in detail the transition from a galactic to an extragalactic origin of cosmic rays thanks to the analysis of super-hybrid coincidences.

AERA has been extended in May 2013 with 100 new stations. With this stage 2, AERA now covers 6 km², which will significantly increase the statistics of UHECR recorded radio signals.

References

- A. Corstanje, M. d. Akker, L. Bühren, H. Falcke, & W. Frieswijk et al. 2011, (2011) arXiv:1109.5805.
- A. Horneffer for the LOPES Collaboration. 2007, Proc. of 30th ICRC (2007) Merida, Mexico
- B Revenu. 2013, AIP Conf. Proc., 1535, 56
- B. Revenu for the Pierre Auger and CODALEMA Collaborations. 2012, Nucl. Instrum. Meth. A 662 (2012) S130
- C. Glaser for Pierre Auger Collaboration. 2013, AIP Conf. Proc., 1535, 68
- D. Ardouin et al. 2005, Nucl. Instrum. Meth. A 555 (2005) 148
- D. Ardouin et al. 2012
- D. Charrier for the CODALEMA Collaboration. 2012, Nucl. Instrum. Meth. A, 662, S142
- D. Torres Machado for the CODALEMA Collaboration. 2013, Proc 33rd ICRC (2013) Rio de Janeiro, Brasil
- F. D. Kahn & I. Lerche. 1966, Proc. Roy. Soc. A 289 (1966) 206.
- G. A. Askaryan. 1962, Soviet Phys. JETP 14 (1962) 441
- H. Falcke et al. 2005, Nature 435 (2005) 313
- H. R. Allan. 1971, Progress in Elementary Particle and Cosmic-Ray Physics 10 (1971) 169, North Holland
- J. Alvarez Muñiz, W. R Carvalho Jr., & E. Zas. 2012, Astropart. Phys. 35 (2012) 325.
- K. D. de Vries, van den Berg, A., O. Scholten, & K. Werner. 2012, Astropart. Phys. 34 (2010) 267.
- K. Weidenhaupt for the Pierre Auger Collaboration. 2012, Proc. Vulcano Workshop (2012) Vulcano, Italy
- K. Werner, de Vries, K., & O. Scholten. 2012, Astropart. Phys. 37 (2012) 5.
- M. Ludwig & T. Huege. 2011, Astropart. Phys. 34 (2011) 438
- M. Melissas for the Pierre Auger Collaboration. 2012, AIP Conf. Proc. 1535 (2013) 63
- O. Ravel for the CODALEMA Collaboration. 2012, Nucl. Instrum. Meth. A 662 (2012) S89
- T. Huege, M. Ludwig, & C. W. James. 2013, AIP Conf. Proc. 1535 (2013) 128.
- T. Huege for the Pierre Auger Collaboration. 2013, Proc 33rd ICRC (2013) Rio de Janeiro, Brasil,
- The Pierre Auger Collaboration, D. Charrier, L. Denis, et al. 2012a, JINST, 7, P10011
- The Pierre Auger Collaboration, S. Acounis, D. Charrier, et al. 2012b, JINST, 7, P11023
- V. Marin & B Revenu. 2012, Astropart. Phys., 35, 733